

Photoswitchable Spiropyran Molecular for Specific Sensing of Thiols and Fluorescent Ink

Tiantian Xu,^a Xu Zhang,^a Qian Wang,^a Shaobing Zhang,^a Chengkun Wang,^a Hui Li,^a Zheng Yang,^{ab} Xiaodan Jia,^{ab} Xiangrong Liu,^{ab}

^a College of Chemistry and Chemical Engineering, Xi'an University of Science and Technology, Xi'an 710054, P. R. China;

^b Key Laboratory of Coal Resources Exploration and Comprehensive Utilization, Ministry of Land and Resources, Xi'an 710012, P. R. China;

*Corresponding author: yangzheng@xust.edu.cn; orcid.org/0000-0002-1554-4794.

CONTENTS

1. The optical properties of probe	S2
2. Calculation of the LODs	
S12	
3. IR, NMR and MS spectra	
S17	
4. MTT assay results of the probe	S23

1. Optical properties of the probe.

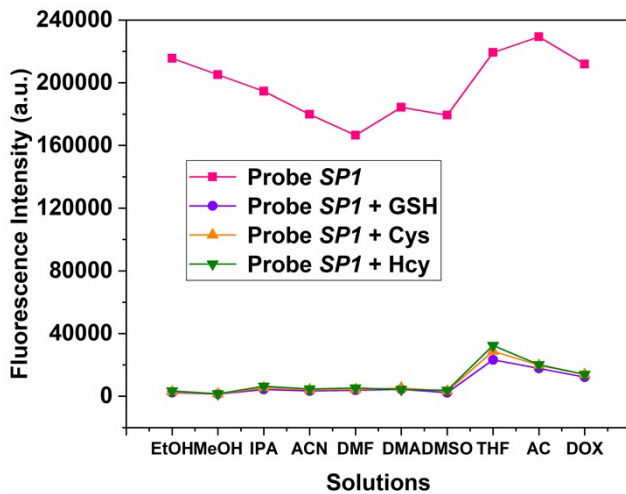


Fig. S1 Fluorescence intensity of probe **SP1** ($20 \mu\text{mol}\cdot\text{L}^{-1}$) in presence of 2.5 equiv. of thiols in different solutions with PBS buffer ($0.2 \text{ mol}\cdot\text{L}^{-1}$, pH 7.4), $\lambda_{\text{ex}} = 370 \text{ nm}$.

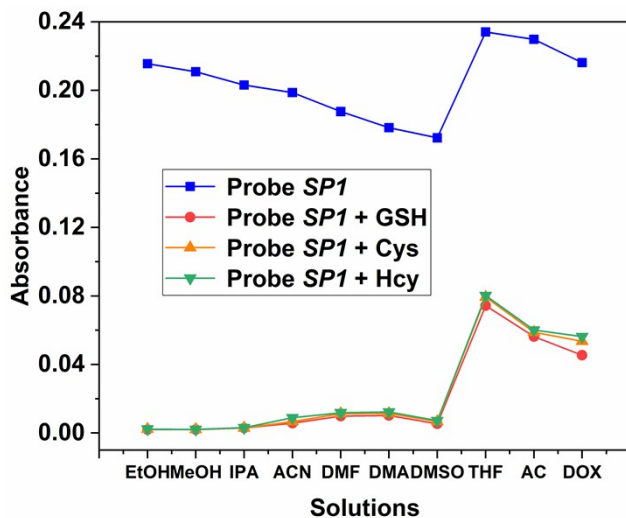


Fig. S2 Absorbance of probe **SP1** ($20 \mu\text{mol}\cdot\text{L}^{-1}$) in presence of 2.5 equiv. of thiols in different solutions with PBS buffer ($0.2 \text{ mol}\cdot\text{L}^{-1}$, pH 7.4).

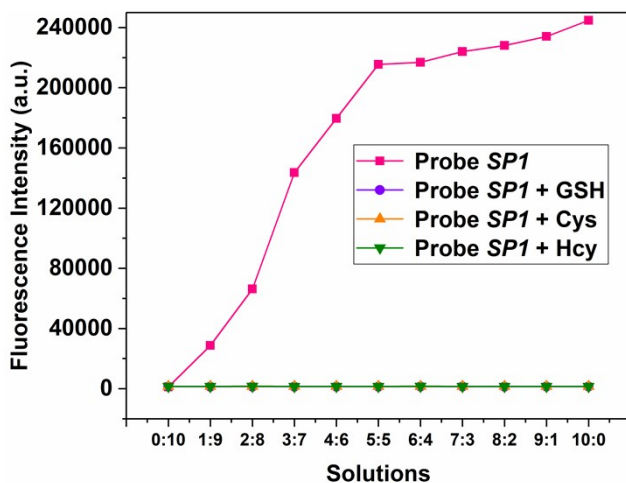


Fig. S3 Fluorescence intensity of probe **SP1** ($20 \mu\text{mol}\cdot\text{L}^{-1}$) in presence of 2.5 equiv. of thiols in different EtOH-H₂O solutions with PBS buffer ($0.2 \text{ mol}\cdot\text{L}^{-1}$, pH 7.4), $\lambda_{\text{ex}} = 370 \text{ nm}$.

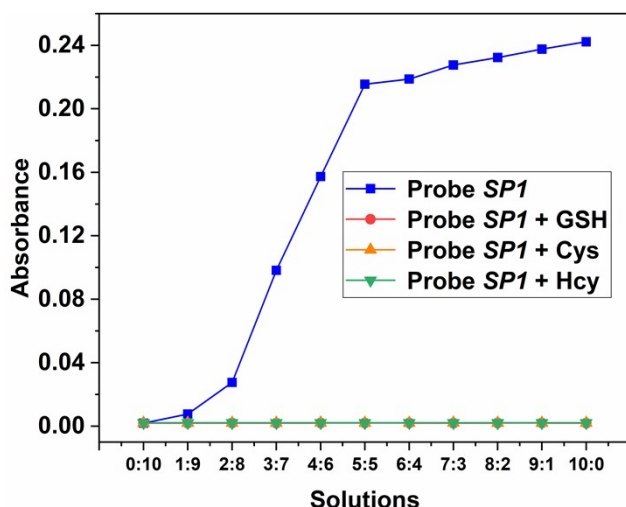


Fig. S4 Absorbance of probe **SP1** ($20 \mu\text{mol}\cdot\text{L}^{-1}$) in presence of 2.5 equiv. of thiols in different EtOH-H₂O solutions with PBS buffer ($0.2 \text{ mol}\cdot\text{L}^{-1}$, pH 7.4).

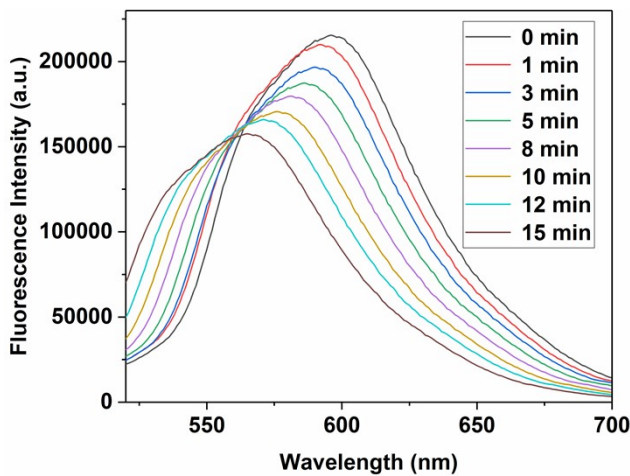


Fig. S5 Fluorescence spectra of the probe *SPI* under continuous heating at 80 °C in EtOH-H₂O (5:5, v/v, PBS, pH 7.4) solution, $\lambda_{\text{ex}} = 370$ nm.

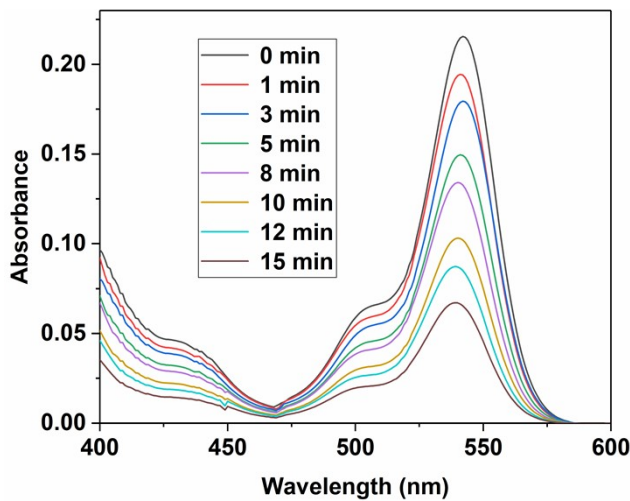


Fig. S6 Absorption spectra of the probe *SPI* under continuous heating at 80 °C in EtOH-H₂O (5:5, v/v, PBS, pH 7.4) solution.

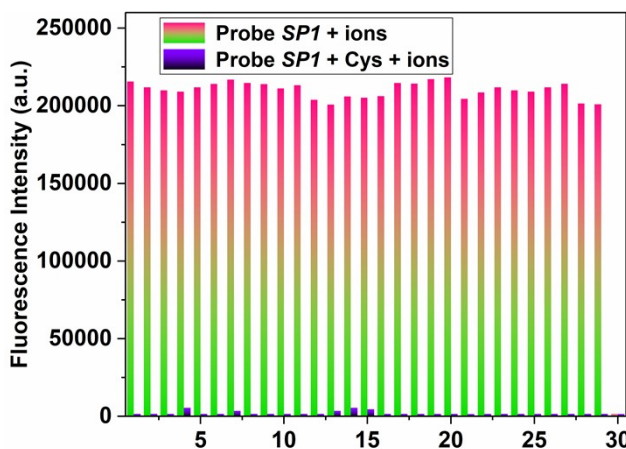


Fig. S7 Fluorescence intensity changes of probe **SP1** ($20 \mu\text{mol}\cdot\text{L}^{-1}$) in EtOH-H₂O (5:5, v/v, PBS, pH 7.4) over the analytes of interest. Pink-green bars represent the fluorescence response of probe **SP1** to: 1, blank; 2, Na⁺; 3, K⁺; 4, Ag⁺; 5, Ca²⁺; 6, Mg²⁺; 7, Cu²⁺; 8, Cd²⁺; 9, Mn²⁺; 10, Co²⁺; 11, Ni²⁺; 12, Zn²⁺; 13, Pb²⁺; 14, Hg²⁺; 15, Fe³⁺; 16, Cr³⁺; 17, Al³⁺; 18, O₂^{·-}; 19, H₂O₂; 20, NO; 21, H₂S; 22, ONOO⁻; 23, NO₃⁻; 24, PO₄³⁻; 25, CO₃²⁻; 26, OAc⁻; 27, C₂O₄²⁻; 28, SO₃²⁻; 29, HClO; 30, Cys. Blue-black bars represent the fluorescence response with subsequent addition of 2.5 equiv. of Cys to the above solutions, $\lambda_{\text{ex}} = 370 \text{ nm}$.

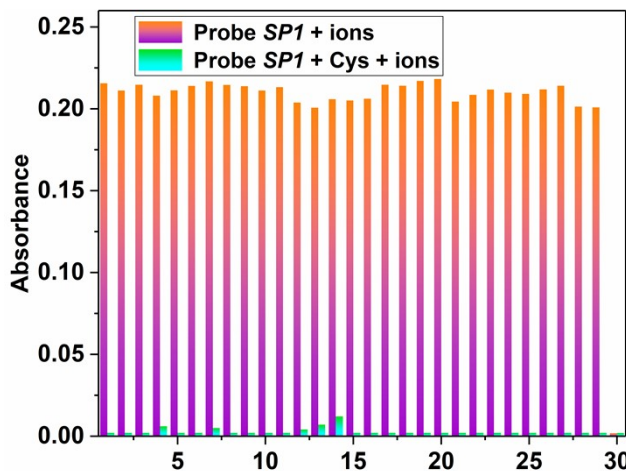


Fig. S8 Absorbance changes of probe **SP1** ($20 \mu\text{mol}\cdot\text{L}^{-1}$) in EtOH-H₂O (5:5, v/v, PBS, pH 7.4) over the analytes of interest. Orange-purple bars represent the fluorescence response of probe **SP1** to: 1, blank; 2, Na⁺; 3, K⁺; 4, Ag⁺; 5, Ca²⁺; 6, Mg²⁺; 7, Cu²⁺; 8, Cd²⁺; 9, Mn²⁺; 10, Co²⁺; 11, Ni²⁺; 12, Zn²⁺; 13, Pb²⁺; 14, Hg²⁺; 15, Fe³⁺; 16, Cr³⁺; 17, Al³⁺; 18, O₂^{·-}; 19, H₂O₂; 20, NO; 21, H₂S; 22, ONOO⁻; 23, NO₃⁻; 24, PO₄³⁻; 25, CO₃²⁻; 26, OAc⁻; 27, C₂O₄²⁻; 28, SO₃²⁻; 29, HClO; 30, Cys. Green-cyan bars represent the fluorescence response with subsequent addition of 2.5 equiv. of Cys to the above

solutions.

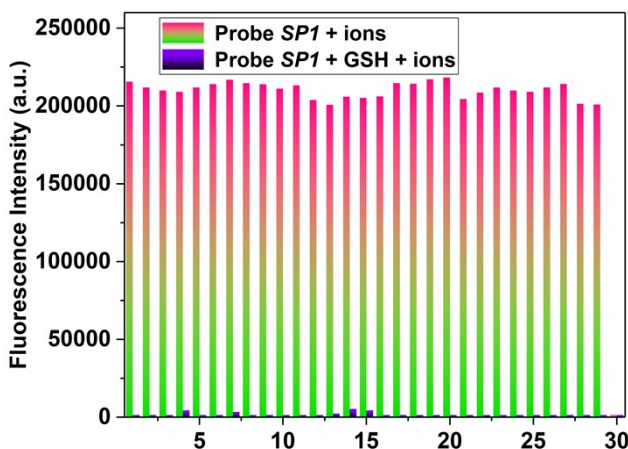


Fig. S9 Fluorescence intensity changes of probe **SP1** ($20 \mu\text{mol}\cdot\text{L}^{-1}$) in EtOH-H₂O (5:5, v/v, PBS, pH 7.4) over the analytes of interest. Pink-green bars represent the fluorescence response of probe **SP1** to: 1, blank; 2, Na⁺; 3, K⁺; 4, Ag⁺; 5, Ca²⁺; 6, Mg²⁺; 7, Cu²⁺; 8, Cd²⁺; 9, Mn²⁺; 10, Co²⁺; 11, Ni²⁺; 12, Zn²⁺; 13, Pb²⁺; 14, Hg²⁺; 15, Fe³⁺; 16, Cr³⁺; 17, Al³⁺; 18, O₂⁻; 19, H₂O₂; 20, NO; 21, H₂S; 22, ONOO⁻; 23, NO₃⁻; 24, PO₄³⁻; 25, CO₃²⁻; 26, OAc⁻; 27, C₂O₄²⁻; 28, SO₃²⁻; 29, HClO; 30, GSH. Blue-black bars represent the fluorescence response with subsequent addition of 2.5 equiv. of GSH to the above solutions, $\lambda_{\text{ex}} = 370 \text{ nm}$.

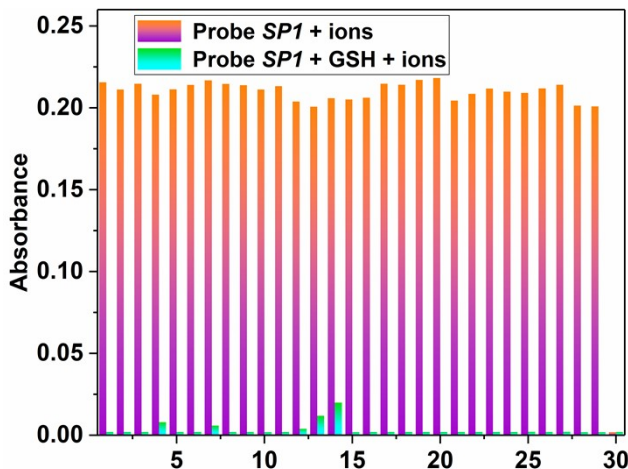


Fig. S10 Absorbance changes of probe **SP1** ($20 \mu\text{mol}\cdot\text{L}^{-1}$) in EtOH-H₂O (5:5, v/v, PBS, pH 7.4) over the analytes of interest. Orange-purple bars represent the fluorescence response of probe **SP1** to: 1, blank; 2, Na⁺; 3, K⁺; 4, Ag⁺; 5, Ca²⁺; 6, Mg²⁺; 7, Cu²⁺; 8, Cd²⁺; 9, Mn²⁺; 10, Co²⁺; 11, Ni²⁺; 12, Zn²⁺; 13, Pb²⁺; 14, Hg²⁺; 15, Fe³⁺; 16, Cr³⁺; 17, Al³⁺; 18, O₂⁻; 19, H₂O₂; 20, NO; 21, H₂S; 22, ONOO⁻; 23, NO₃⁻; 24, PO₄³⁻; 25, CO₃²⁻; 26, OAc⁻; 27, C₂O₄²⁻; 28, SO₃²⁻; 29, HClO; 30, GSH. Green-cyan bars represent the fluorescence response with subsequent addition of 2.5 equiv. of GSH to the above solutions, $\lambda_{\text{ex}} = 370 \text{ nm}$.

of GSH to the above solutions.

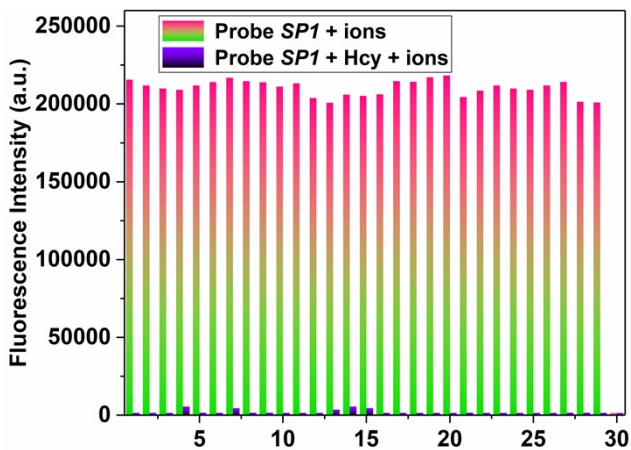


Fig. S11 Fluorescence intensity changes of probe **SPI** ($20 \mu\text{mol}\cdot\text{L}^{-1}$) in EtOH-H₂O (5:5, v/v, PBS, pH 7.4) over the analytes of interest. Pink-green bars represent the fluorescence response of probe **SPI** to: 1, blank; 2, Na⁺; 3, K⁺; 4, Ag⁺; 5, Ca²⁺; 6, Mg²⁺; 7, Cu²⁺; 8, Cd²⁺; 9, Mn²⁺; 10, Co²⁺; 11, Ni²⁺; 12, Zn²⁺; 13, Pb²⁺; 14, Hg²⁺; 15, Fe³⁺; 16, Cr³⁺; 17, Al³⁺; 18, O₂⁻; 19, H₂O₂; 20, NO; 21, H₂S; 22, ONOO⁻; 23, NO₃⁻; 24, PO₄³⁻; 25, CO₃²⁻; 26, OAc⁻; 27, C₂O₄²⁻; 28, SO₃²⁻; 29, HClO; 30, Hcy. Blue-black bars represent the fluorescence response with subsequent addition of 2.5 equiv. of Hcy to the above solutions, $\lambda_{\text{ex}} = 370 \text{ nm}$.

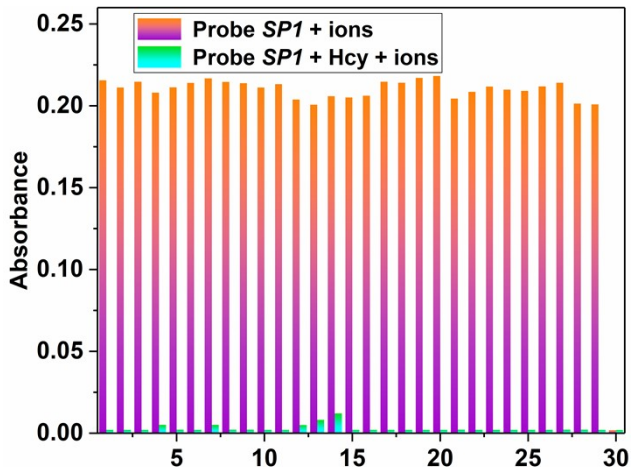


Fig. S12 Absorbance changes of probe **SPI** ($20 \mu\text{mol}\cdot\text{L}^{-1}$) in EtOH-H₂O (5:5, v/v, PBS, pH 7.4) over the analytes of interest. Orange-purple bars represent the fluorescence response of probe **SPI** to: 1, blank; 2, Na⁺; 3, K⁺; 4, Ag⁺; 5, Ca²⁺; 6, Mg²⁺; 7, Cu²⁺; 8, Cd²⁺; 9, Mn²⁺; 10, Co²⁺; 11, Ni²⁺; 12, Zn²⁺; 13, Pb²⁺; 14, Hg²⁺; 15, Fe³⁺; 16, Cr³⁺; 17, Al³⁺; 18, O₂⁻; 19, H₂O₂; 20, NO; 21, H₂S; 22, ONOO⁻; 23, NO₃⁻; 24, PO₄³⁻; 25, CO₃²⁻; 26, OAc⁻; 27, C₂O₄²⁻; 28, SO₃²⁻; 29, HClO; 30, Hcy. Green-cyan bars represent the fluorescence response with subsequent addition of 2.5 equiv. of

Hcy to the above solutions.

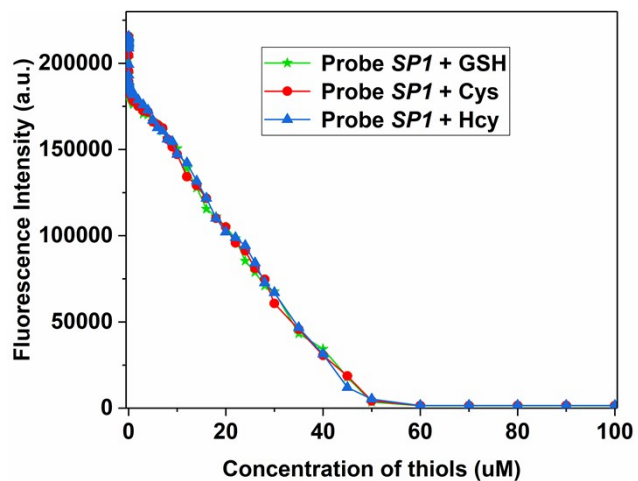


Fig. S13 Fluorescence intensity change of probe *SP1* ($20 \mu\text{mol}\cdot\text{L}^{-1}$) in EtOH-H₂O (5:5, v/v, PBS, pH 7.4) solution as a function of thiols concentration at 596 nm, $\lambda_{\text{ex}} = 370 \text{ nm}$.

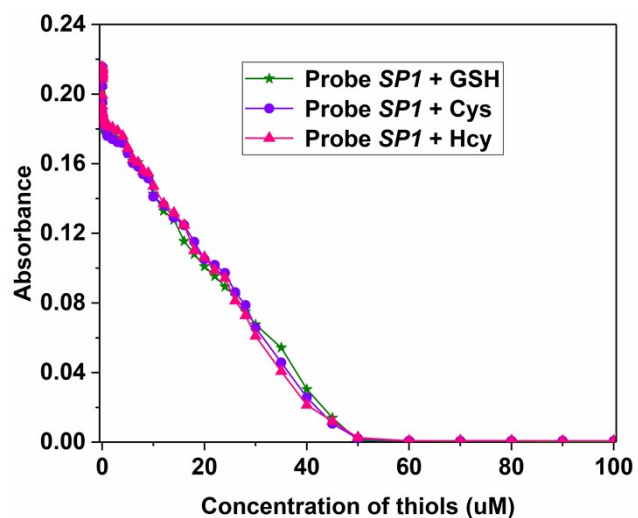


Fig. S14 Absorption intensity change of probe *SP1* ($20 \mu\text{mol}\cdot\text{L}^{-1}$) in EtOH-H₂O (5:5, v/v, PBS, pH 7.4) solution as a function of thiols concentration at 542 nm.

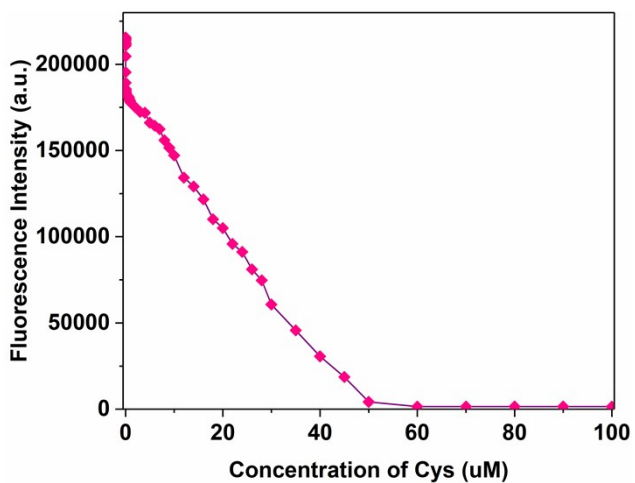


Fig. S15 Fluorescence intensity change of probe *SP1* ($20 \mu\text{mol}\cdot\text{L}^{-1}$) in EtOH-H₂O (5:5, v/v, PBS, pH 7.4) solution as a function of Cys concentration at 596 nm, $\lambda_{\text{ex}} = 370 \text{ nm}$.

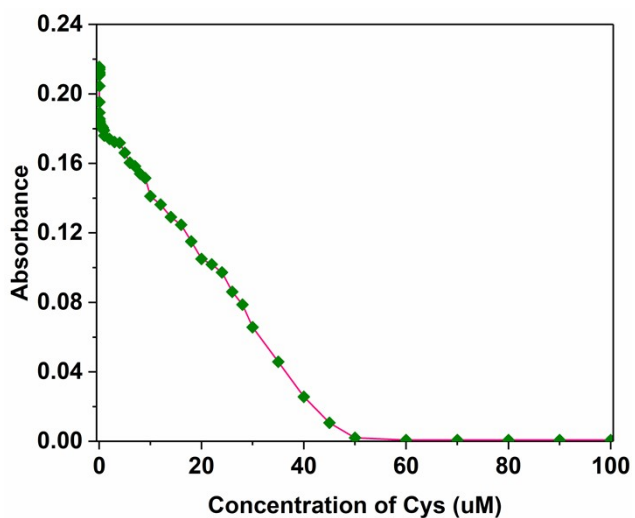


Fig. S16 Absorption intensity change of probe *SP1* ($20 \mu\text{mol}\cdot\text{L}^{-1}$) in EtOH-H₂O (5:5, v/v, PBS, pH 7.4) solution as a function of Cys concentration at 542 nm.

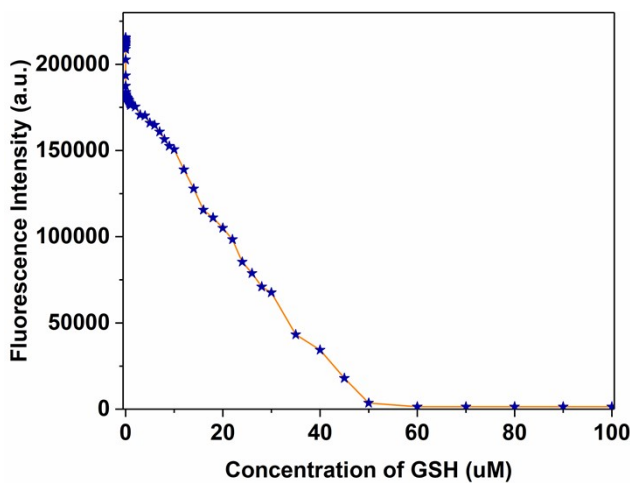


Fig. S17 Fluorescence intensity change of probe *SP1* ($20 \mu\text{mol}\cdot\text{L}^{-1}$) in EtOH-H₂O (5:5, v/v, PBS, pH 7.4) solution as a function of GSH concentration at 596 nm, $\lambda_{\text{ex}} = 370 \text{ nm}$.

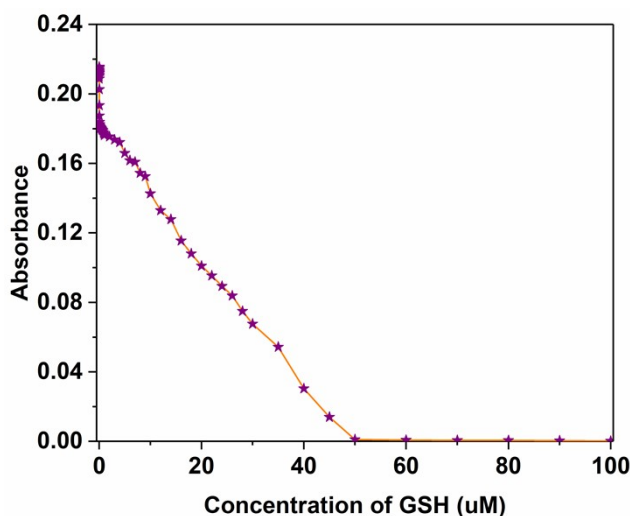


Fig. S18 Absorption intensity change of probe *SP1* ($20 \mu\text{mol}\cdot\text{L}^{-1}$) in EtOH-H₂O (5:5, v/v, PBS, pH 7.4) solution as a function of GSH concentration at 542 nm.

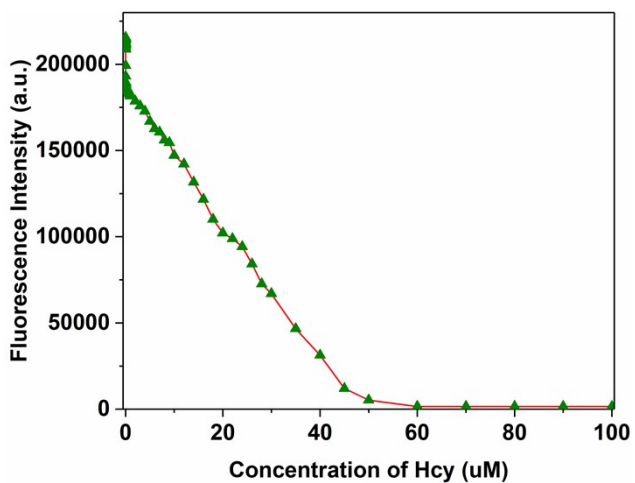


Fig. S19 Fluorescence intensity change of probe *SP1* ($20 \mu\text{mol}\cdot\text{L}^{-1}$) in EtOH-H₂O (5:5, v/v, PBS, pH 7.4) solution as a function of Hcy concentration at 596 nm, $\lambda_{\text{ex}} = 370 \text{ nm}$.

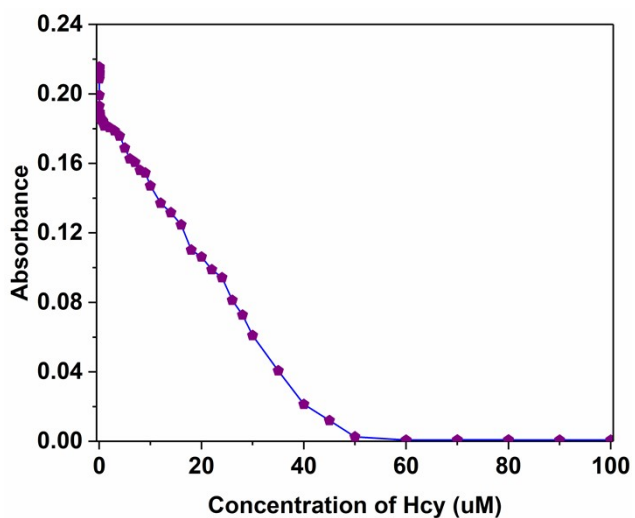


Fig. S20 Absorption intensity change of probe *SP1* ($20 \mu\text{mol}\cdot\text{L}^{-1}$) in EtOH-H₂O (5:5, v/v, PBS, pH 7.4) solution as a function of Hcy concentration at 542 nm.

2. Calculation of the LODs.

The detection limits were estimated based on the Kaiser's definition:

$$y_d = y_b - KS_b \text{ (on-off)}$$

y_d is the detection limit of the sample. y_b present the mean value fluorescence intensity of the blank samples. S_b is the population standard deviation of the blank.

The K value is 3 (M. Belter, A. Sajnog, D. Baralkiewicz, *Tlanta*, 2014, **129**, 606.).

Table S1. Fluorescence intensity and the Standard deviation of the blank samples

	Fl. Intensity	Mean value	Standard deviation	$y_d = y_b - KS_b$
Blank #1	215570			
Blank #2	214022			
Blank #3	216852			
Blank #4	214642			
Blank #5	213894			
Blank #6	214683	214900	1218	211247
Blank #7	214190			
Blank #8	217148			
Blank #9	213915			
Blank #10	214087			

[a] y_d is the detection limit of the sample. y_b present the mean value fluorescence intensity of the blank samples. S_b is the population standard deviation of the blank.

The K value is 3.

Table S2. Fluorescence intensity and corresponding concentration of thiols

[Thiols] ($\mu\text{mol}\cdot\text{L}^{-1}$ ¹⁾)	FL. Intensity (Cys)	FL. Intensity (GSH)	FL. Intensity (HCy)
0.001	215570	215570	215570
0.002	215362	215112	215362
0.003	215051	215001	215051
0.004	214412	214912	214412
0.005	213947	213947	213947
0.006	212637	213137	212637
0.007	212312	212312	212312
0.008	211861	211861	211861
0.009	211436	210936	211436
0.01	211062	210062	211062
0.02	210825	208738	210041
0.03	204643	202616	208735
0.04	195368	193434	199276
0.05	189281	187407	193066
0.06	185670	183832	189383
0.07	185508	183671	189218
0.08	184396	182571	188084
0.09	183602	181784	187274
0.1	183105	181292	186767

Table S3. Comparison of *SP1* for information encryption with other reported methods.

Material	Advantage	Ref.
Organic molecular (pyrene derivatives)	Orthogonal and temporal encryption properties	11
Organic molecular (Purine derivatives)	High fluorescence quantum yield, brightness, optical stability	12
Organic molecular (cyanostilbene derivatives)	Photostability, simple preparation process and processability	13
Tetraphenylethylene@graphene oxide	Switchable microstructure and fluorescence	14
perylene diimide-based metallacages	High quantum yield, white-light emission	15
Upconversion nanoparticles	Excellent dispersibility and good stability	16
Fluorescent polymeric nanoparticles	With tunable FRET efficiency, good photoreversibility, excellent fluorescence stability	17
Fluorescent Polymers	Color-tunable properties and dual-mode luminescence	18
AIE-CDs	Aggregation fluorescence and acid-sensitive	19
F, NCDs@SiO ₂	Thermally activated delayed fluorescence	20
Organic molecular (spiropyran)	Photoswitching performance, high fluorescence quantum yield, optical stability, stimuli-responsive and color-tunable property	This work

Table S4. Comparison of sensing platforms for the detection of biothiols.

Materials	Methods	Linear range ($\mu\text{mol}\cdot\text{L}^{-1}$)	LOD ($\mu\text{mol}\cdot\text{L}^{-1}$)	Response time (min)	Ref.
Organic molecular (Rhodamine B)	Fluorometry	0-12	GSH: 5.15		
		0-12	Cys: 0.865	20 min	1
		0-12	Hcy: 6.51		
Organic molecular (fluorescent dye JSC)	Fluorometry	0-8	GSH: 0.0042		
		0-5	Cys: 0.0079	-	2
		0-30	Hcy: 0.0102		
Organic molecular (xanthene derivative)	Fluorometry	0-4	GSH: 0.0095		
		0.5-4.5	Cys: 0.0048	-	3
		0-1.5	Hcy: 0.0062		
Organic molecular (quinoxaline)	Fluorometry	1-7	GSH: 0.0571	180 min	
		1-8	Cys: 0.0366	30 min	4
		1-10	Hcy: 0.1165	180 min	
AuNCs@ZIF-8	Fluorometry	1.5-8	GSH: 0.32		
		1-10	Cys: 0.15	10 min	5
poly(thymine)- templated copper nanoparticles	Fluorometry	0-10	GSH: 0.015		
		0-10	Cys: 0.0125	10 min	6
		0-10	Hcy: 0.02		
DNA-templated silver nanoclusters-Hg ²⁺ system	Fluorometry	0.04-0.1	GSH:		
		0.02-0.1	0.00288	-	7
			Cys: 0.00159		
Nanocluster of copper and silver	Fluorometry /colorimetry	20-80	Cys: 7.0	-	8
		20-520	GSH:		
Carbon dot	Fluorometry	5-580	0.02039	-	9
		Hcy:80-360	Cys: 0.00931		

			Hcy: 0.00193		
		5-200	GSH: 1.7		
Carbon dots	Fluorometry	5-100	Cys: 2.3	-	10
		5-225	Hcy: 3.0		
Organic molecular (spiropyran)		0.1-50	GSH: 0.0074		This work
	Fluorometry	0.1-50	Cys: 0.0086	<1min	
		0.1-50	Hcy: 0.0082		

3. IR, NMR and MS spectra.

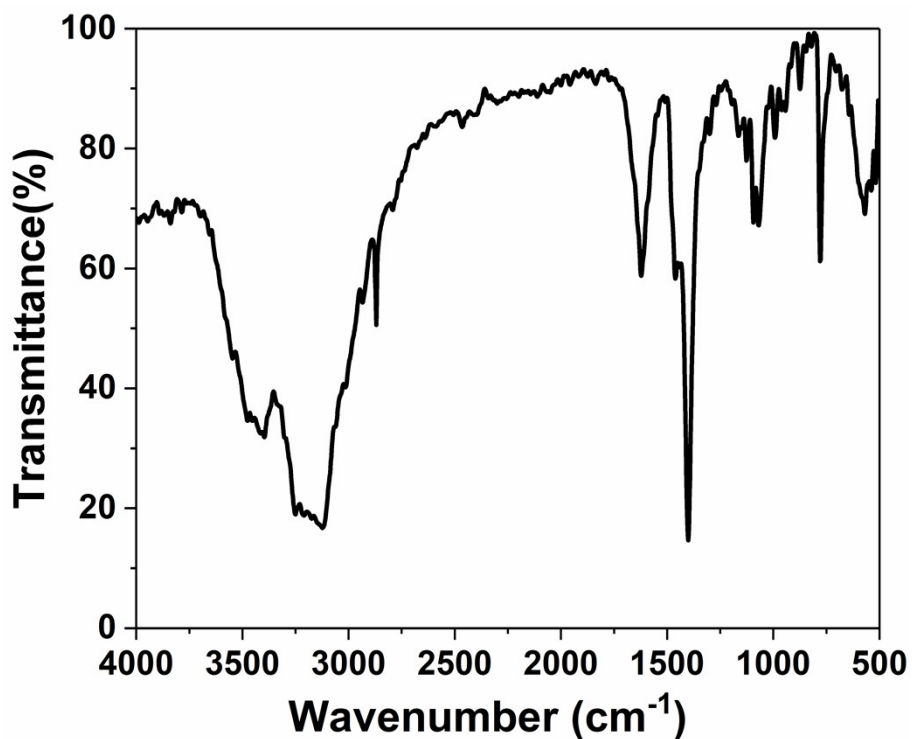


Fig. S21 IR spectrum of compound 1 in KBr.

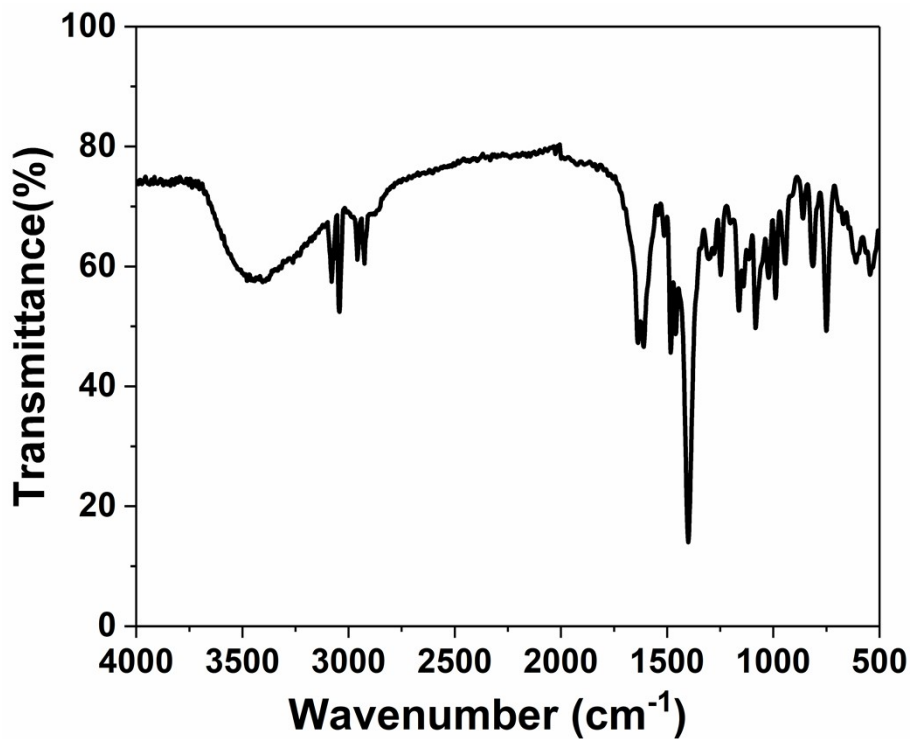


Fig. S22 IR spectrum of compound 2 in KBr.

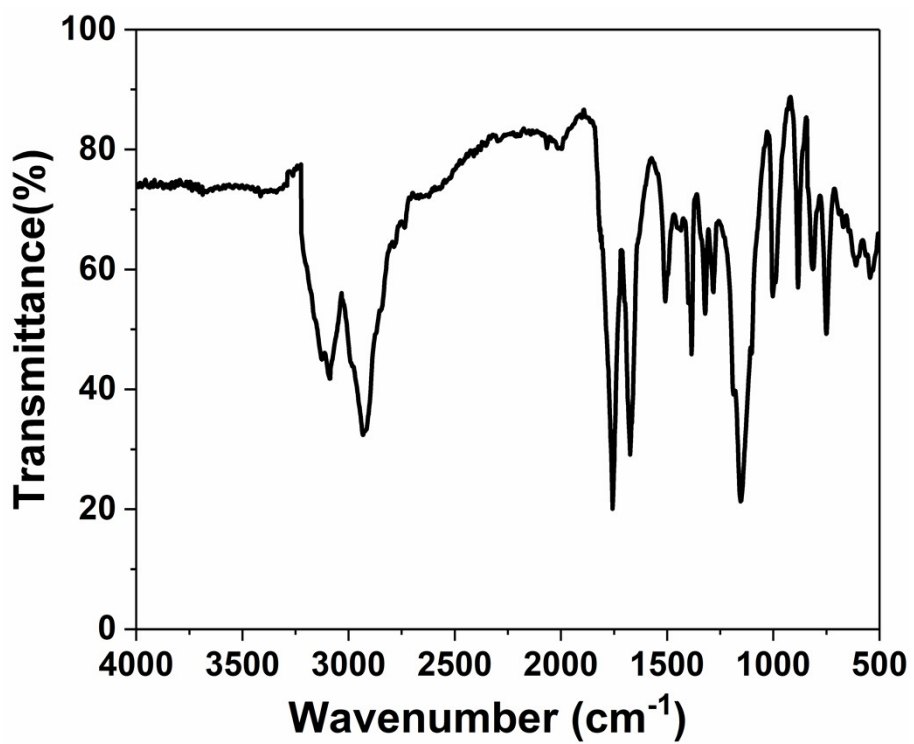


Fig. S23 IR spectrum of probe *SPI* in KBr.

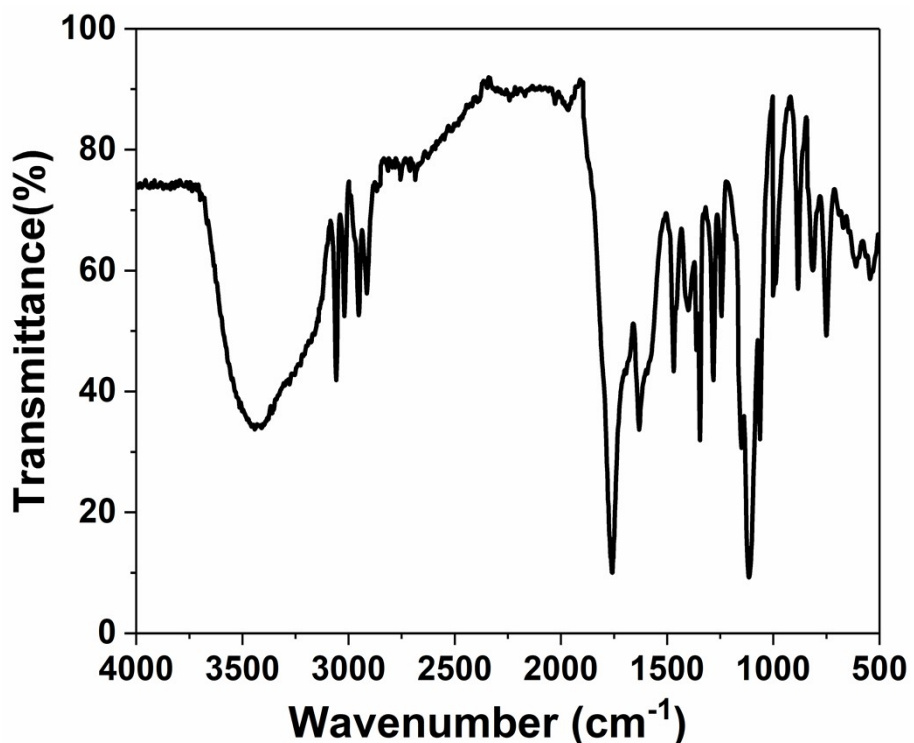


Fig. S24 IR spectrum of probe *SPI* + Cys in KBr.

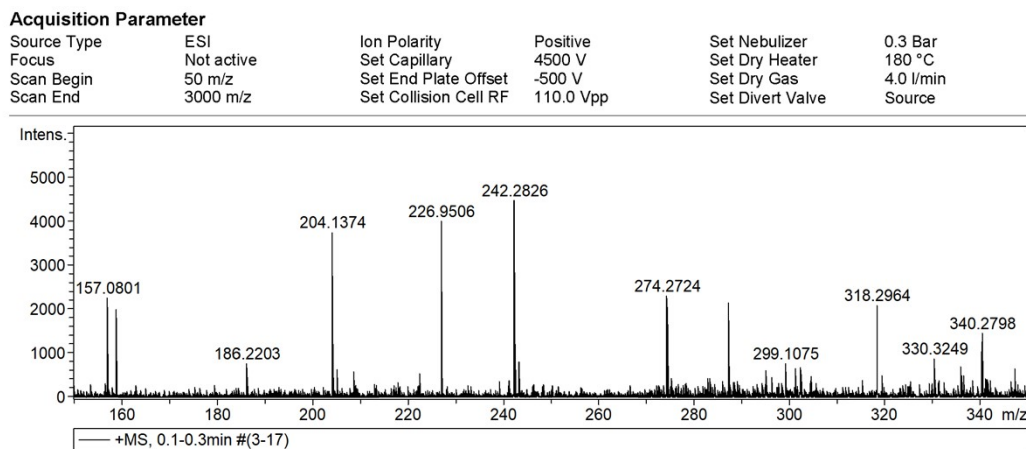


Fig. S25 Mass spectrum of compound 1.

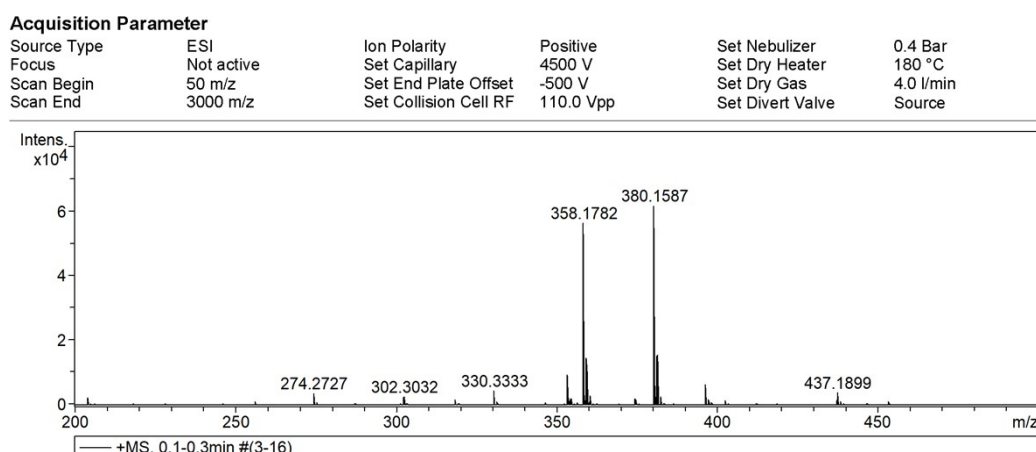


Fig. S26 Mass spectrum of compound 2.

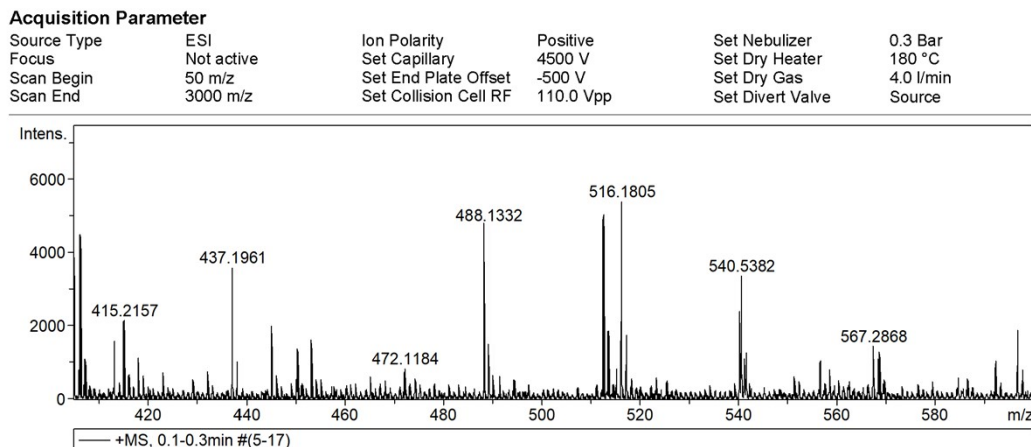


Fig. S27 Mass spectrum of probe **SPI**.

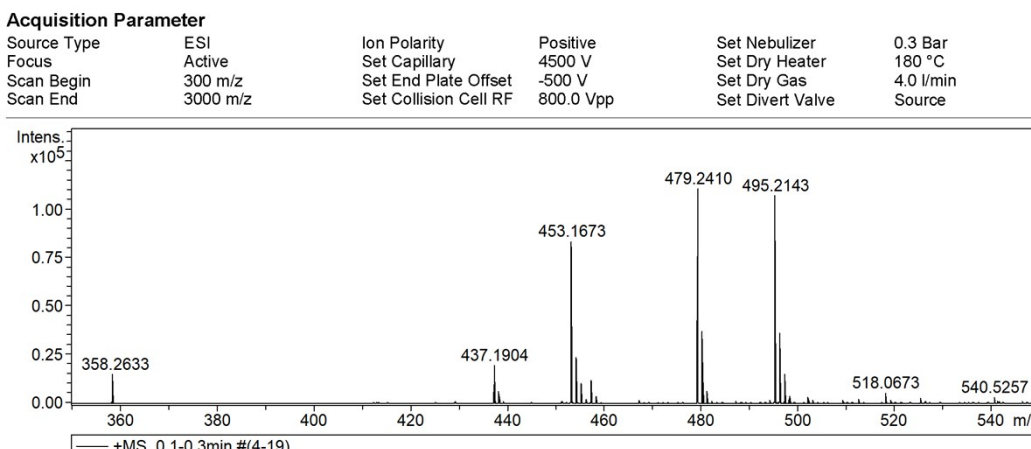


Fig. S28 Mass spectrum of probe **SPI** + Cys.

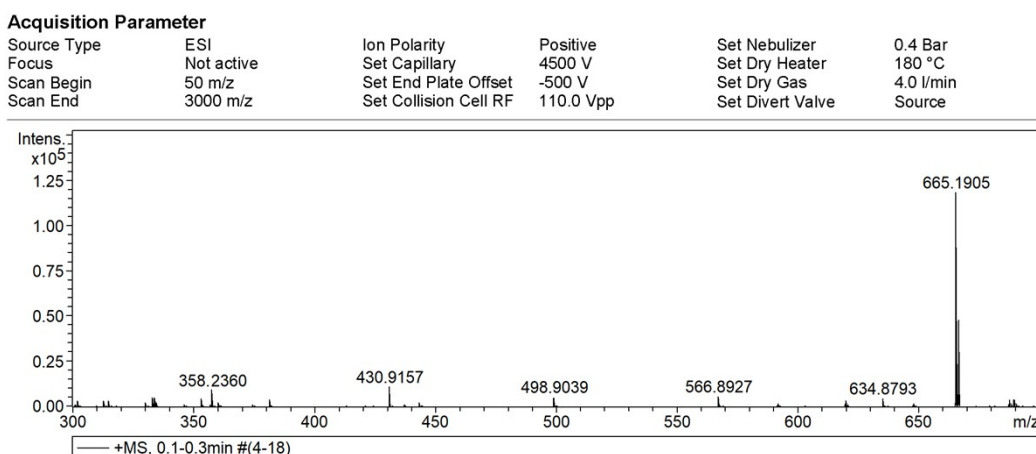


Fig. S29 Mass spectrum of probe **SPI** + GSH.

Acquisition Parameter

Source Type	ESI	Ion Polarity	Positive	Set Nebulizer	0.4 Bar
Focus	Not active	Set Capillary	4500 V	Set Dry Heater	180 °C
Scan Begin	50 m/z	Set End Plate Offset	-500 V	Set Dry Gas	4.0 l/min
Scan End	3000 m/z	Set Collision Cell RF	110.0 Vpp	Set Divert Valve	Source

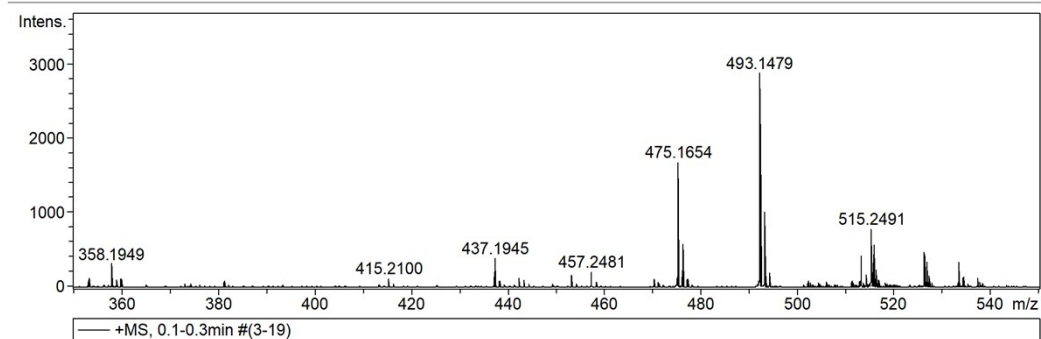


Fig. S30 Mass spectrum of probe **SPI** + Hcy.

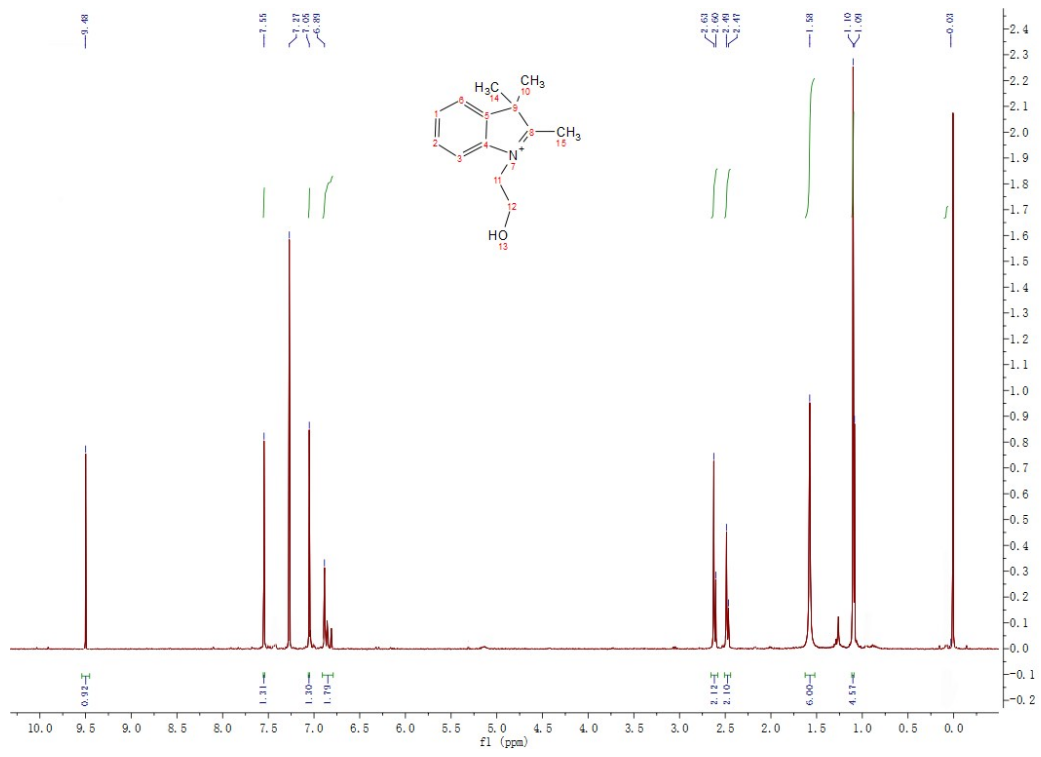


Fig. S31 ^1H NMR spectrum of compound **1** in CDCl_3 .

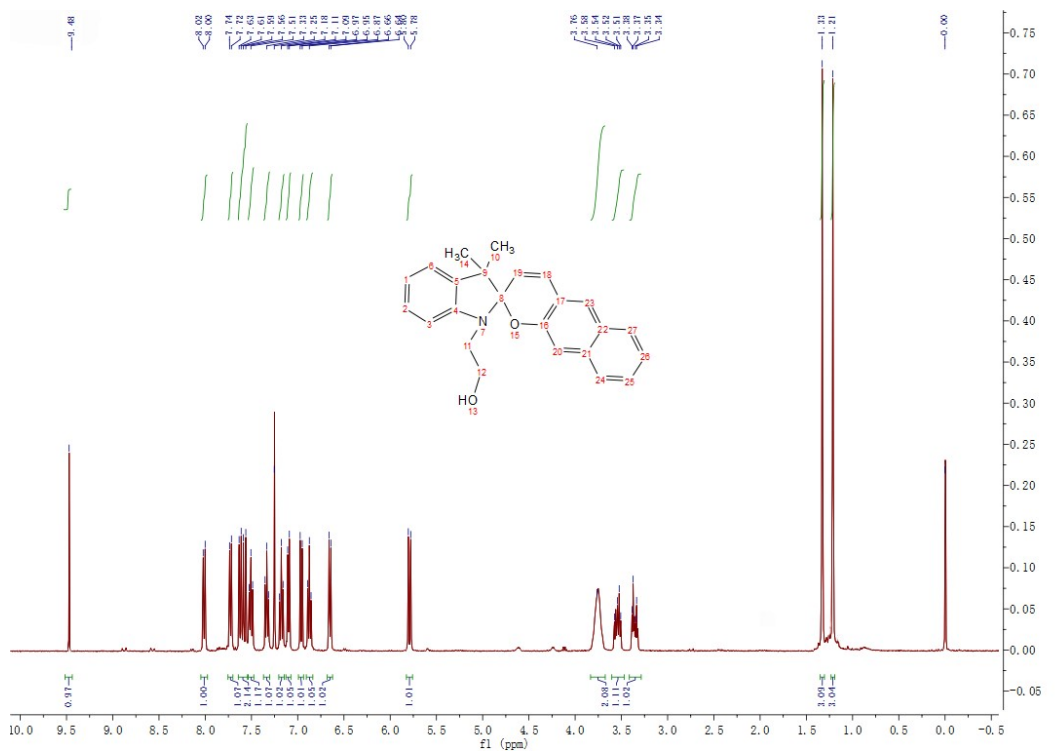


Fig. S32 ^1H NMR spectrum of compound 2 in CDCl_3 .

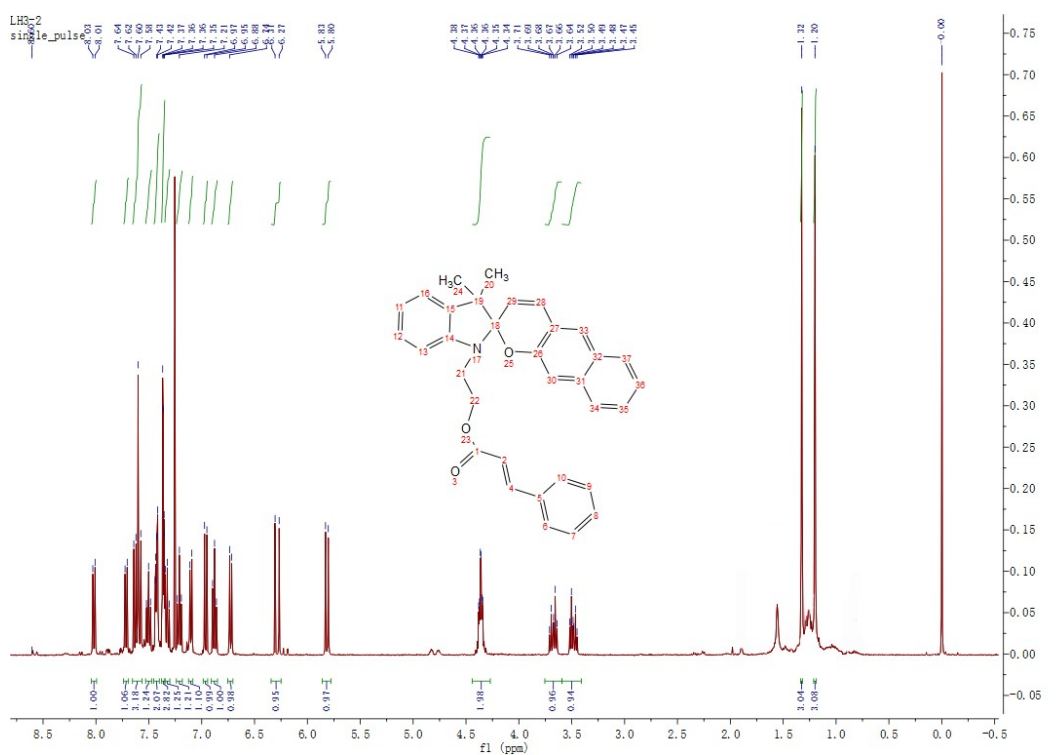


Fig. S33 ^1H NMR spectrum of probe SPI in CDCl_3 .

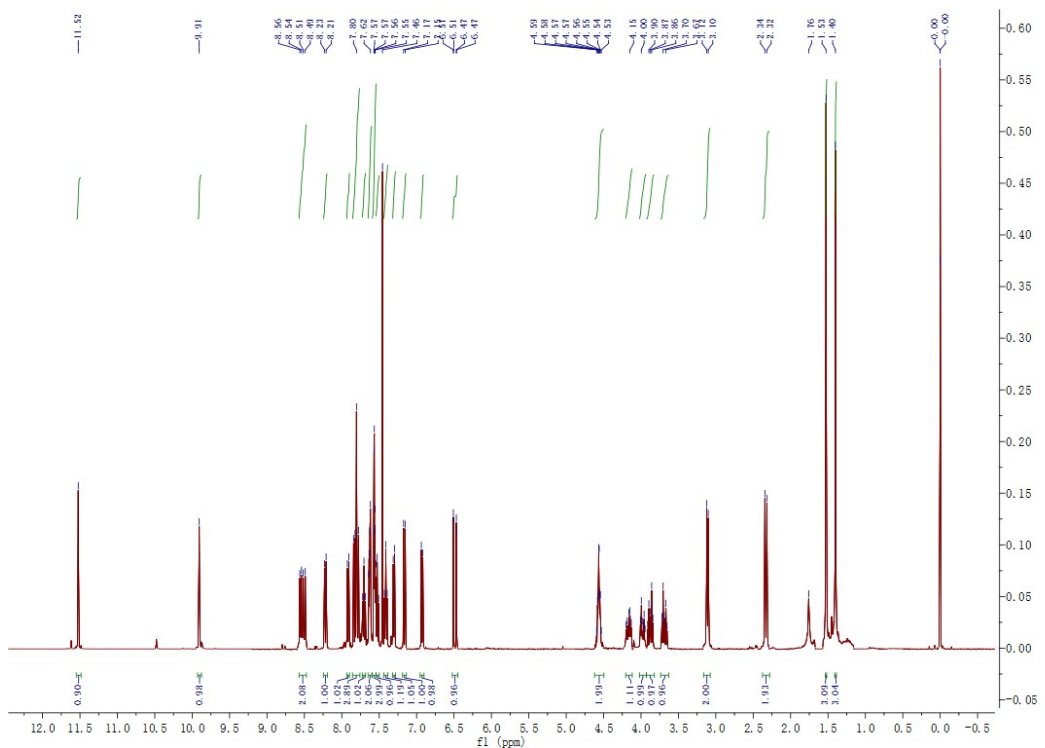


Fig. S34 ^1H NMR spectrum of probe *SPI* + Cys in CDCl_3 .

4. MTT assay results of the probe.

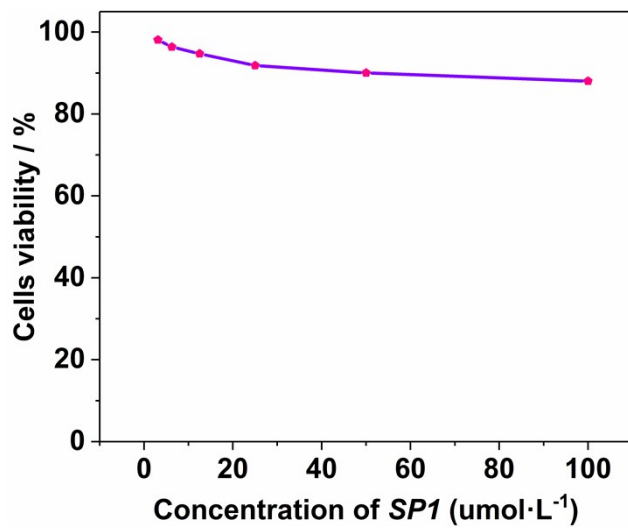


Fig. S35. The influence of cell viability with the change of *SPI* concentration.

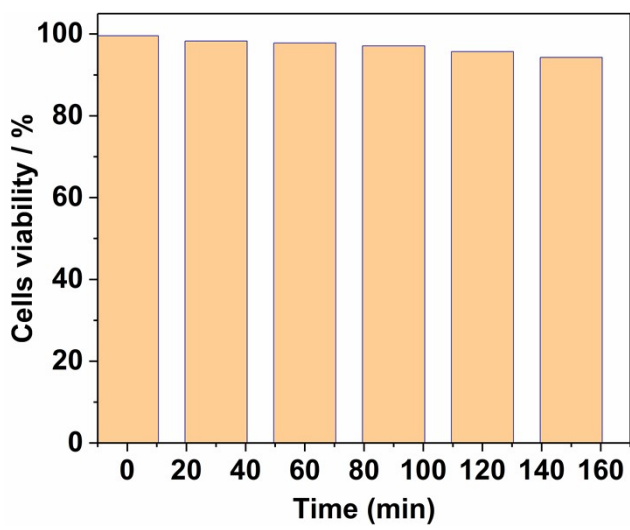


Fig. S36. The relationship between cell viability and incubation time.

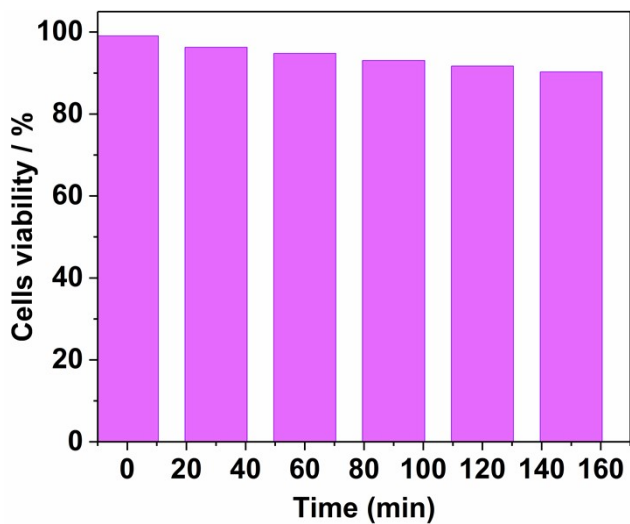


Fig. S37. The relationship between cell viability and incubation time in addition of 20 $\mu\text{mol}\cdot\text{L}^{-1}$ of *SPI*.

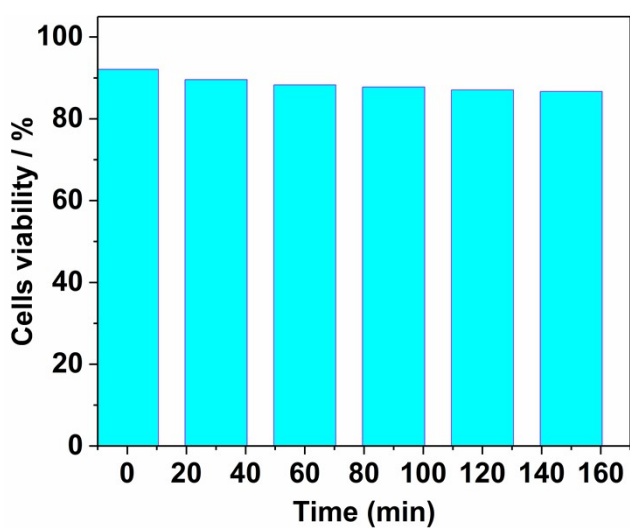


Fig. S38. The relationship between cell viability and incubation time in addition of 20 $\mu\text{mol}\cdot\text{L}^{-1}$ of **SPI** and 2.5 equiv. of Cys.

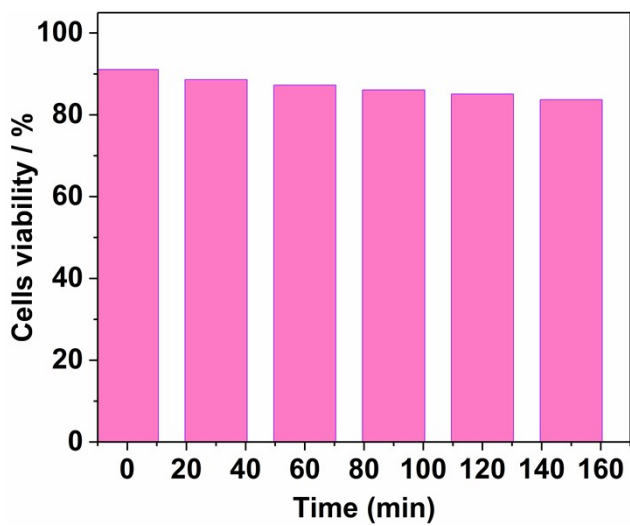


Fig. S39. The relationship between cell viability and incubation time in addition of 20 $\mu\text{mol}\cdot\text{L}^{-1}$ of **SPI** and 2.5 equiv. of GSH.

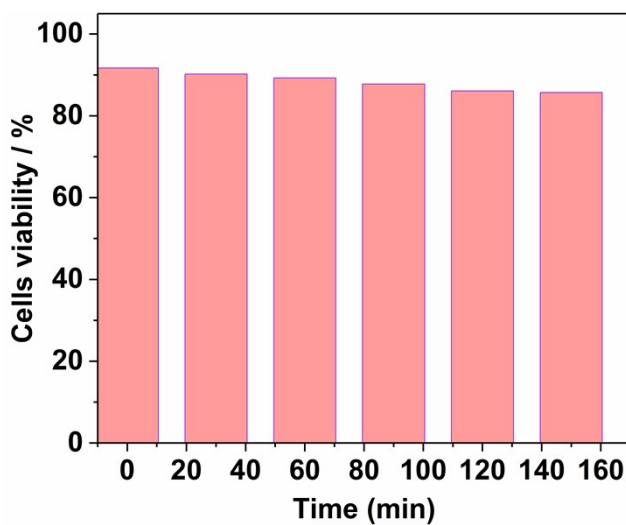


Fig. S40. The relationship between cell viability and incubation time in addition of 20 $\mu\text{mol}\cdot\text{L}^{-1}$ of *SPI* and 2.5 equiv. of Hcy.

Table S5. MTT assay results, calculated inhibition ratio and IC₅₀ value of the probe *SPI* for MG-63 cell.

[<i>SPI</i>]/ μM	1	2	3	Average	Inhibition ratio	IC ₅₀ / μM
3.125	0.443	0.463	0.455	0.4537	0.0188	
6.25	0.448	0.455	0.434	0.4457	0.0361	
12.5	0.432	0.434	0.448	0.4380	0.0527	
25	0.416	0.426	0.432	0.4247	0.0816	>100
50	0.412	0.414	0.423	0.4163	0.0996	
100	0.372	0.387	0.362	0.3737	0.1919	